



Contents lists available at [ScienceDirect](http://www.sciencedirect.com)

Aeolian Research

journal homepage: www.elsevier.com/locate/aeolia



Windblown sand saltation: A statistical approach to fluid threshold shear velocity



Lorenzo Raffaele ^{a,d,*}, Luca Bruno ^{b,d}, Franco Pellerrey ^c, Luigi Preziosi ^{c,d}

^a Politecnico di Torino, Department of Structural, Geotechnical and Building Engineering, Corso Duca degli Abruzzi 24, I-10129 Torino, Italy

^b Politecnico di Torino, Department of Architecture and Design, Viale Mattioli 39, I-10125 Torino, Italy

^c Politecnico di Torino, Department of Mathematical Sciences, Corso Duca degli Abruzzi 24, I-10129 Torino, Italy

^d Windblown Sand Modeling and Mitigation Joint Research Group, Italy

ARTICLE INFO

Article history:

Received 15 January 2016

Revised 3 October 2016

Accepted 10 October 2016

Keywords:

Windblown sand

Saltation

Fluid threshold shear velocity

Uncertainty

Statistics

Copula modelling

ABSTRACT

The reliable prediction in probabilistic terms of the consequences of aeolian events related to sand transport phenomena is a key element for human activities in arid regions. Threshold shear velocity generating sand lifting is a key component of such a prediction. It suffers from the effect of uncertainties of different origin, such as those related to the physical phenomena, measurement procedures, and modelling. Semi empirical models are often fitted to a small amount of data, while recent probabilistic models need the probability distribution of several random variables. Triggered by this motivation, this paper proposes a purely statistical approach to fluid threshold shear velocity for sand saltation, treated as a single comprehensive random variable. A data set is derived from previously published studies. Estimates of conditional probability distributions of threshold shear velocity for given grain diameters are given. The obtained statistical moments are critically compared to some deterministic semi empirical models refitted to the same collected data. The proposed statistical approach allows to obtain high order statistics useful for practical purposes.

© 2016 Elsevier B.V. All rights reserved.

1. Introduction

Aeolian sand transport is a complex process that is induced by the interaction between subfields such as wind, air suspended particles and bed-particles. It contributes to soil erosion and landform evolution. Understanding and modelling its features is of fundamental interest in many research fields. Beside the importance of windblown sand and dust in Earth sciences (Kok et al., 2012), from the engineering perspective, simulating windblown sand phenomena is relevant because of the interaction with a number of human activities and related infrastructures in arid environments (e.g. Middleton and Sternberg, 2013; Rizvi, 1989; Alghamdi and Al-Kahtani, 2005; Zhang et al., 2007; Cheng and Xue, 2014). In the infrastructure design perspective and within a probabilistic approach to design, the engineer is interested in relating a sand erosion or transport condition to a given, preferably low enough,

probability of exceedance, i.e. in defining a high percentile sand transport rate.

Among the transport mechanisms responsible of sand transport, saltation largely prevails in terms of sand mass. The evaluation of the involved sand flux is usually given in terms of sand transport rate by several laws, revised for example in Dong et al. (2003), Kok et al. (2012) and Sherman and Li (2012). Most of such laws require the definition and evaluation of an erosion threshold, i.e. the minimum value of the wind shear stress at which saltation occurs. Usually, such a threshold is given in terms of threshold values of the shear velocity and depends on a number of parameters belonging to both the wind and the sand. Since the seminal work of Bagnold (1941), two threshold shear velocities have been recognized: the fluid or static threshold, defined as the minimum wind speed for initiation of sediment transport without antecedent transport, and the dynamic or impact threshold, i.e. the minimum wind speed for sustaining sediment transport with the presence of transport. Most studies proposing transport laws in steady saturated flow refer to the impact threshold (Kok et al., 2012). Hence fundamental studies (e.g. Andreotti, 2004; Pahtz et al., 2012; Kok, 2010) recently proposed models of the impact threshold in light of a few number of experimental measures, e.g. Bagnold (1937), Chepil (1945), Tsoar et al. (1994) and Li et al. (2014).

* Corresponding author at: Politecnico di Torino, Department of Structural, Geotechnical and Building Engineering, Corso Duca degli Abruzzi 24, I-10129 Torino, Italy.

E-mail address: lorenzo.raffaele@polito.it (L. Raffaele).

URL: <http://www.polito.it/wsmm> (L. Raffaele).

However, the impact threshold shear velocity is approximated for application purposes as equal about 80% of the fluid threshold one (e.g. Bagnold, 1937; Pye and Tsoar, 2009; Zheng, 2009; Kok et al., 2012). Reference to the fluid threshold shear velocity is motivated by the long-standing and wide literature reviewed by Shao (2008), Pye and Tsoar (2009), Merrison (2012) and Kok et al. (2012) and summarized in the following. In the rest of the paper, we address to the fluid threshold shear velocity as “threshold shear velocity” u_{*t} for the sake of compactness.

Systematic experimental measurements of u_{*t} versus the grain diameter were carried out by Bagnold (1937), Chepil (1945), Zingg (1953), Fletcher (1976) and Iversen et al. (1976) amongst others. These measurements constitute the consolidated literature data base. They are reported in Fig. 1 versus the equivalent particle diameter d_{eq} (Chepil, 1951; Kok et al., 2012). A significant scatter among data can be observed notably at low values of the particle diameter. However, two general trends can be observed, divided by a local minimum at about 75–100 μm (Kok et al., 2012).

A number of deterministic models of the threshold shear velocity have been proposed in literature so far. They can be categorized in two classes with respect to both modelling scale and goal. Microscopic models discuss the equilibrium of the moments of the forces acting on the single particle resting on a bed of other particles (Shao, 2008). They aim at pointing out the physical phenomena underlying each force and at modelling it. In a general framework, entraining aerodynamic forces (drag and lift ones) induce saltation, while stabilizing forces (gravitational and the interparticle ones) counteract them (Greeley and Iversen, 1985; Shao and Lu, 2000). On one hand, the effective gravitational force including buoyancy, and the drag force correspond to well known phenomena and their modelling is widely accepted, see e.g. Greeley and Iversen (1985) and the cited reviews. On the other hand, the same does not hold for the other forces: the resultant lift force results from the Saffman one (Saffman, 1965) and the lift induced by vortical structures; the overall interparticle force results from several kinds of forces, including van der Waals forces, water adsorption forces and electrostatic forces. Although interparticle forces are expected to scale with the soil particle size (e.g. Shao and Lu, 2000), their modelling for aspherical and rough sand and dust remains poorly understood (Kok et al., 2012). In particular, such forces depend upon a number of parameters such as surface cleanliness, surface roughness at micro/nano meter scale, air and grain humidity, mineralogy and surface contaminants affecting hydrophilicity (Merrison, 2012). Semi-empirical macroscopic models aim at approximating the threshold shear velocity trend versus the particle diameter. Some of them are compared to the experimental data

in Fig. 1(a). Because of the above modelling difficulties, they do not analytically include the contribution of lift and interparticle forces while they explicitly retain the gravitational and drag ones. Any other contribution is accounted for in a semi empirical approach by introducing one or more free parameter(s), and the value of the latter obtained by fitting experimental data. The pioneering model by Bagnold (1941) involves a single dimensionless constant A_B , resulting independent from the grain diameter or, in other terms, from Reynolds number. Then, it gives rise to a monotonic increasing trend of $u_{*t}(d)$. The model by Iversen and White (1982) defines the same parameter $A(\text{Re}_{*t})$ as a piece-wise empirical function of the friction Reynolds number Re_{*t} to mimic the effects of lift and interparticle forces: the resulting $u_{*t}(d)$ law is no longer monotonic and qualitatively reflect the trend of the experimental data. The model by Shao and Lu (2000) is more compact than the previous one. It neglects the Re_{*t} dependency, and at the same time generalizes the Bagnold one by introducing a novel correction term to account for the interparticle forces. A second dimensional constant free parameter γ [N/m] is included in the correction term. More recently, McKenna (2003) has considered the effect of soil moisture on the interparticle cohesive force by defining $\gamma(\Delta P, d)$ as a function of the capillary-suction pressure deficit and of the grain diameter. Other laws of u_{*t} have been proposed for natural surfaces: they account for the effects of soil texture, soil moisture, salt concentration, surface crust, vegetation and/or pebbles on the surface. The review of such models is out of the scopes of the present paper. Interested readers can refer to Shao (2008) and Webb and Strong (2011).

Although the deterministic approach largely prevails in aeolian literature, the view that the threshold velocity should be regarded as a statistical phenomenon may be dated back to the pioneering studies by Chepil (1945). The probabilistic modelling approach is motivated by the scatter of the experimental data at low values of d even for a common nominal setup condition (Fig. 1-a), and by the difficulties experienced by the deterministic approach, i.e. the challenge of parameterizing threshold variability and relating this variability to its different sources.

The randomness of bed grain geometry and of the turbulent wind flow have been early recognized as sources of threshold variability in the experimental studies of Nickling (1988) and Williams et al. (1990, ?), respectively. In particular, the wind tunnel tests by Nickling (1988) first showed that measured fluid and impact thresholds could not be reproduced, presumably because it is impossible to replicate grain positioning between each test. In fact, most sediment is composed of a range of grain sizes and shapes. Thus, for a given surface, variability is expected due to the

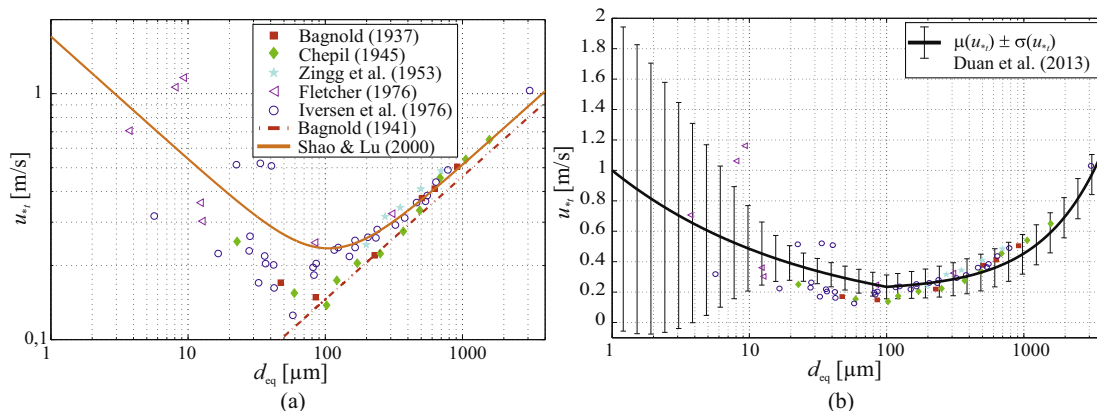


Fig. 1. Threshold friction velocity: experimental data (symbols) compared with semi-empirical deterministic models (a, redrawn after Kok et al., 2012), and the probabilistic model by Duan et al. (2013) (b).

positioning of sediment grains. Since the positioning of grains affects their susceptibility to entrainment, the fluid or impact threshold for a given surface is not easily described by a single value (Lancaster and Nickling, 1994). Values of u_{*t} were found to span an unexpectedly wide range for each grain fraction during the wind tunnel tests by Williams et al. (1990, 1994). Such a variability was conjectured to be due to the effects of turbulent flow regimes changing in space and time. They obtained approximations of the probability density function for u_{*t} required for future stochastic treatment of the threshold condition. More recently, both the randomness of bed grain geometry and of the turbulent wind flow have been included in the probabilistic models proposed by Wu and Chou (2003) and Zhen-shan et al. (2008). Conceptually, both studies agree that the initial movement of sand grains should be regarded as a random phenomenon and probabilistic models of entrainment could provide better understanding of it. Technically, both probabilistic models are microscopic ones, limited to ideal spherical particles, and do not consider random interparticle forces. However, the studies differ in their results and conclusions: Zhen-shan et al. (2008) propose a probabilistic reading of the conventional threshold friction velocity, while Wu and Chou (2003) separately derive the probability of entrainment in the rolling and lifting mode, and call into question the consistency embedded in the conventional definition of the critical shear stress for incipient motion, following the remarks by other authors (see review by McEwan and Heald, 2001).

The randomness of the *interparticle forces* and their effects of the threshold variability have been first recognized by Zimon (1982). He suggested to treat cohesive forces acting upon dust particles as random variables (r.v.s). He argued from experimental data that their probability distribution can be approximated by a lognormal one. Following Zimon's findings, Shao (2008) has recently assumed that also the threshold shear velocity of dust particles is a log-normally distributed r.v. It is worth pointing out that such an assumption looks questionable from an analytical point of view even by assuming that the cohesive force is the sole random variable among the grain acting forces. In fact, u_{*t} does not result from a simple rescaling of the cohesive force. The smaller the grain size is, the bigger the role of the interparticle forces is, the higher the expected effect of the their uncertainties on the threshold shear velocity is. Having this qualitative dependency in mind, Shao (2008) conjectured that the obtained results do not hold for sand-sized particles, for which threshold shear velocity can be still defined as a deterministic quantity. It is worth pointing out that the discontinuous switch from a probabilistic model for dust to a deterministic one for sand seems questionable having in mind that the diameter is a continuous quantity and the relative effects of interparticle forces are expected to be continuously decreasing with it.

Even more recently, the effects of the random nature of the *soil surface microstructure* and of the *irregular shape of the particles* have been included in a probabilistic model for threshold shear velocity by Duan et al. (2013). The proposed microscopic model describes the moments induced by gravitational, electrostatic, cohesion, and drag forces as functions of four microscopic r.v.s. The threshold shear velocity is then expressed as a function of these random quantities, some of them independent, some dependent. Its probability density function is then evaluated through a statistical estimation of the distributions of the predictors. Subsequently, the mean value and standard deviation of the threshold shear velocity are fitted as functions of d . The obtained results (Fig. 1-b) are not entirely convincing. First, the standard deviation $\sigma(u_{*t})$ is monotonically increasing for $d \geq 100 \mu\text{m}$ and asymptotically tends to 0.132, while the scatter of experimental data clearly decreases for increasing d . Second, the mean $\mu(u_{*t})$ is a linear function of d

for $d > 100 \mu\text{m}$, while its deterministic counterpart, i.e. the nominal values obtained by semi-empirical macroscopic models, is not. In our opinion, such critical features can be ascribed to both modelling and technical difficulties. Among the former ones, the challenging task in writing a microscopic model inclusive of all the r.v.s affecting the sand grain acting forces. Among the latter ones, the difficulties in obtaining probability distribution for each microscopic r.v. from measurements and in handling mutually dependent r.v.s.

In the conclusion of their paper Wu and Chou (2003) rise the issue of not yet investigated effects of other random factors on the probabilities of sediment entrainment. To our best knowledge, a comprehensive categorization of such random factors is not given in Aeolian Research. However, sources of uncertainty have been conceptually introduced (e.g. in Halpern, 2003; Zio and Pedroni, 2013) and systematically reviewed in related disciplines, including Environmental Modelling (Refsgaard et al., 2007; Uusitalo et al., 2015), Physical Geography (Foley, 2010), Ecology (Regan et al., 2002), Wind Energy (Yan et al., 2015). Having in mind that erosion belongs to the general class of environmental problems (Uusitalo et al., 2015), in the following the uncertainty classification proposed for the latter is applied to the former.

Uncertainty is defined as the lack of exact knowledge, regardless of what is the cause of this deficiency (Refsgaard et al., 2007). Uncertainty stems from various sources. Overlapping uncertainty classifications can be found in literature, the typology varying remarkably depending on the context and scope (see the reviews cited above). Nevertheless, every taxonomy reflects a common general classification (Zio and Pedroni, 2013) that distinguishes between *aleatory* and *epistemic* uncertainty. The former refers to inherent randomness of natural phenomena. The latter is associated with the lack of knowledge about the properties and conditions of the phenomena to be modeled. In the following, published papers dealing with threshold shear velocity uncertainties are briefly reviewed accordingly to this general classification.

- *Aleatory uncertainty*. To the Authors' best knowledge, the scientific literature in Aeolian Research is primarily focused on aleatory uncertainties. They can be further divided referring to the sand and wind subsystems:
 - *Sand uncertainties*. Beside the grain shape, its surface microstructure (Duan et al., 2013), and its relative position with respect to the other bed particles (Nickling, 1988), other uncertainties at the grain scale affect the grain mineralogy and its surface cleanliness (Merrison, 2012). At the macroscopic scale, the *grain size distribution* is traditionally recognized in literature as an important sand feature affecting u_{*t} (e.g. Edwards and Namikas, 2015 and included references), beside the mean diameter. In fact, smaller particles interspersed among the large particles provide additional cohesive forces in natural sands, resulting in higher threshold conditions (Roney and White, 2004). The early studies on u_{*t} (e.g. Bagnold, 1937) usually assume nominally uniform sand, but this restriction clearly does not hold in a probabilistic framework;
 - *Wind uncertainties*. Beside the ones due to the turbulent flow (Williams et al., 1994), other uncertainties follows from the inborn variability and/or partially uncontrolled *environmental conditions* even in wind tunnel facilities, e.g. air temperature and air relative humidity (e.g. Greeley and Iversen, 1985; Jones et al., 2002);
- *Epistemic uncertainty*. To the Authors' best knowledge, such a class of uncertainties is explicitly addressed less often in the Aeolian Research literature. It can be further refined as follows:

- *Model uncertainties*, that is uncertainty in the necessarily simplified representation of the behaviour of the natural system, in terms of uncertainty in the identification and definition of the variables, hypotheses assumed, interactions left out, and shapes of the functions. With regard to u_{*t} models, first a single quantitative definition of the same “fluid threshold” is not shared in aeolian community. The lack of a shared definition is highlighted by e.g. Shao (2008), Swann et al. (2015) and Burr et al. (2015). Early qualitative definitions suffered the fact that grain motion initiates intermittently in time and not uniformly in space: Bagnold (1941) refers to the “complete bed motion”; Iversen et al. (1976) refers to “the lowest ... speed at which the majority of exposed particles ... are set in motion” and “general motion of the exposed particles”; Greeley et al. (1976) to “movement of particles over the entire bed”; Iversen and White (1982) to “continuous motion throughout the bed”; Lyles and Krauss (1971) establish four velocity thresholds respectively related to the motion of the first grain, or of few grains moving intermittently, gusts moving intermittently or general bed motion. Quantitatively, u_{*t} is commonly set to the value at which a small percentage of grains start to move. According to Shao (2008) “inevitably, the practical estimation of u_{*t} involves a certain degree of subjectivity in deciding what is a small percentage”. For instance, in Dong et al. (2003) “the wind is considered to reach the initiation threshold when more than 5 particles were stuck on the sticky tape”. Burr et al. (2015) observe “five stages of grain motion, namely first motion, flurries, patches, motion of $\approx 50\%$ of the longitudinally central portion of the bed, and motion of $\approx 100\%$ of the bed” and finally define threshold as 50% of the bed in motion. The ensemble of the above qualitative and subjective estimates results in an overall source of uncertainty. Second, microscopic models proposed in literature differ in the interparticle cohesive forces accounted for (e.g. van der Waals, electrostatic, capillary, chemical binding, Coulomb forces; Shao, 2008) and in their dependency on particle diameter, linear in theory according to Shao (2008), but scaling with $d^{4/3}$ according to Claudin and Andreotti (2006).
- *Measurement uncertainties*, due to measurements errors and/or to different kind of measurements procedures. Such uncertainties affects both the measurement procedures and techniques adopted to evaluate the bulk granulometry (Blott and Pye, 2006; Zhang et al., 2014), and/or the threshold shear velocity itself (Barchyn and Hugenholtz, 2011; Poortinga et al., 2014). In fact, the sediment transport can be measured by visual observation (Bagnold, 1941), camera monitoring equipment (Williams et al., 1994), impact sensors (Ravi et al., 2004), laser based detection systems (Nickling, 1988), or bimodal slope method (Gillette et al., 1998). Results from these methods are not directly comparable and are significantly scattered (e.g. in Roney and White, 2004);
- *Parameter uncertainties* in the (fixed but poorly known) values of the parameters of a model. For instance, the value of the single parameter of Bagnold (1941) model of fluid threshold friction velocity slightly varies among authors for the same nominal conditions (air flow, nearly uniform sand grains of diameters greater or equal to 0.2 mm): $A = 0.10$ in Bagnold (1937), $0.09 \leq A \leq 0.11$ in Chepil (1945), $A \approx 0.12$ in Zingg (1953), $0.17 \leq A \leq 0.20$ in Lyles and Krauss (1971).

In our opinion, four main questions rise from the state of art briefly reviewed above: i. How to describe the threshold shear

velocity by accounting for the sources of uncertainties introduced above? ii. How can such a description meet the practical engineering need of accurate definition of extreme percentiles of u_{*t} ? iii. How many information about the variability of u_{*t} does the deterministic approach neglect? iv. How to overcome the difficulties encountered by probabilistic mechanical models of u_{*t} in handling a number of microscopic r.v.s?

The present study aims at contributing to shed some light on such issues. The deterministic approach is critically reconsidered in the light of a huge collection of experimental measurements. Then, a purely statistical approach to threshold shear velocity is proposed, where the effects of all kinds of uncertainty sources are comprehensively included and merged. Finally, the two approaches are compared.

The paper develops according to the above objectives through the following sections. In Section 2 the collected measurements and the resulting ensemble of selected data are described. In Section 3 some semi-empirical macroscopic models are refitted to the ensemble by means of non-linear regression. In Section 4 the statistical description of the threshold shear velocity is given by referring to copula-based quantile regression. The deterministic and statistical approach are critically compared in Section 5, while conclusions and research perspectives are outlined in Section 6.

2. Data collection and ensemble setting

The data already collected in Fig. 1 are complemented by additional experimental measures collected from review papers (Kok et al., 2012; Edwards and Namikas, 2015), and studies addressed to the evaluation of sand transport rate for single particle diameters. Table 1 lists in chronological order the considered studies. For each of them, the number # of the tested samples is given: an overall collection of 133 setups follows. All studies test nominally dry granular matters. For each setup, the cited papers provide the grain mean, or median, diameter. Except for Fletcher (1976) and Iversen et al. (1976), granular matter is sand and/or dust grains. In order to account for the effect of different densities ρ of the grain constitutive material, the equivalent particle diameter $d_{eq} = d\rho/\rho_s$ (Chepil, 1951; Kok et al., 2012) is evaluated, where ρ_s

Table 1
Collected studies: Reference, number of samples, reference diameter.

	#	d [mm]
Bagnold (1937)	6	$0.05 \leq d \leq 0.92$
Chepil (1945)	11	$0.02 \leq d \leq 1.57$
Kawamura (1951)	2	0.25, 0.31
Zingg (1953)	5	$0.20 \leq d \leq 0.72$
Chepil (1959)	5	$0.20 \leq d \leq 0.72$
Belly (1964)	1	0.44
Kadib (1964)	1	0.15
Lyles and Krauss (1971)	3	$0.24 \leq d \leq 0.72$
Fletcher (1976)	7	$0.01 \leq d \leq 0.31$
Iversen et al. (1976)	33	$0.01 \leq d \leq 3.09$
Logie (1981)	4	$0.15 \leq d \leq 0.43$
Logie (1982)	1	0.24
Horikawa et al. (1983)	1	0.28
Tian (1988)	3	$0.11 \leq d \leq 0.55$
McKenna Neuman (1989)	3	$0.19 \leq d \leq 0.51$
Darwish (1991)	5	$0.22 \leq d \leq 1.3$
Nalpanis et al. (1993)	2	0.12, 0.19
Nickling and McKenna Neuman (1997)	1	0.20
Dong et al. (2002)	9	$0.13 \leq d \leq 0.90$
Dong et al. (2003)	9	$0.13 \leq d \leq 0.90$
Niño et al. (2003)	5	$0.038 \leq d \leq 0.53$
Cornelis and Gabriels (2004)	3	$0.16 \leq d \leq 0.36$
McKenna Neuman (2004)	1	0.27
Roney and White (2004)	12	$0.31 \leq d \leq 0.39$

is the density of the quartz sand. In Table 1 and in the following the equivalent reference diameter is noted as d for the sake of conciseness.

The complete ensemble of retained sand experimental measurements of u_{*t} is plotted in Fig. 2 versus d . On the one hand, the dependency of u_{*t} on d is qualitatively confirmed over the ensemble. On the other hand, a significant dispersion of the data can be easily observed, notably for small and medium sand diameters. In other terms, u_{*t} takes different values at the same d . This feature suggests that setup uncertain/uncontrolled/not detailed parameters other than d affect u_{*t} . As anticipated in Section 1, such uncertainties belong to both aleatory uncertainty of the physical setup and epistemic uncertainty. They are detailed in the following for the considered studies.

- In the selected setups the *grain size distribution* is often qualitatively described, e.g. “as uniform as possible” in Bagnold (1937), “very well and poorly sorted” in Belly (1964), “naturally graded” in Kawamura (1951). Such a qualitative description is usually complemented by the nominal size-range of grains (e.g. Bagnold, 1937; Dong et al., 2003), while in some papers the cumulative grain size distribution is plotted (e.g. Belly, 1964; Nalpanis et al., 1993; Kawamura, 1951; Nicking and McKenna Neuman, 1997; Roney and White, 2004). Recently, Edwards and Namikas (2015) have made an effort to evaluate a measure of the diameter variability by evaluating the sorting coefficient for a number of studies. In spite of some difficulties in obtaining such a measure from nominal size-range, it is worth recalling that non negligible variability (e.g. sorting ≈ 0.05 , coefficient of variation *c.o.v.* ≈ 0.12 in Chepil (1959)) results also from sieving addressed to obtain sands as uniform as possible. Even greater variability characterizes natural sands (e.g. sorting ≈ 0.65 , *c.o.v.* ≈ 0.35 in Kawamura (1951)). Other randomness

of the grain features (e.g. grain shape, surface microstructure, grain position relative to the other bed particles, grain mineralogy) are not specified in the collected studies.

- *Air humidity* during wind tunnel tests is given and systematically addressed only by Kadib (1964) to our best knowledge.
- The *quantitative definition of the threshold shear velocity* is not commonly adopted in all the studies. Only Lyles and Krauss (1971) provide several u_{*t} values from visual observations depending on the kind of grain motion.
- Analogously, *u_{*t} measurements and post processing techniques* are heterogeneous among the studies (Blott and Pye, 2006; Zhang et al., 2014). Only Roney and White (2004) prove their effects on threshold shear velocity by adopting three different techniques.

The present paper is devoted to the characterization of threshold shear velocity of sand only. Hence, setups adopting dust, i.e. having $d < 0.063$ mm according to ISO14688 (2002), are discarded (empty light grey markers in Fig. 2). It is worth noting that “very coarse” sand ($d > 1.2$ mm) as defined by Friedman and Sanders (1978) is not included in the sand ensemble because of the scarceness of available experimental data. An overall sand ensemble having $\# = 109$ results.

3. Deterministic approach: non-linear regression

Prior to the statistical analysis of the ensemble above, non-linear regression is applied to the collected data in order to refit some of the semi-empirical macroscopic models available in literature. The refitting objective is twofold: on the one hand, the field of application is limited to sands, i.e. on a physics of entrainment relatively simpler than that governing dusts; on the other hand, model parameters are fitted to a number of data higher than that

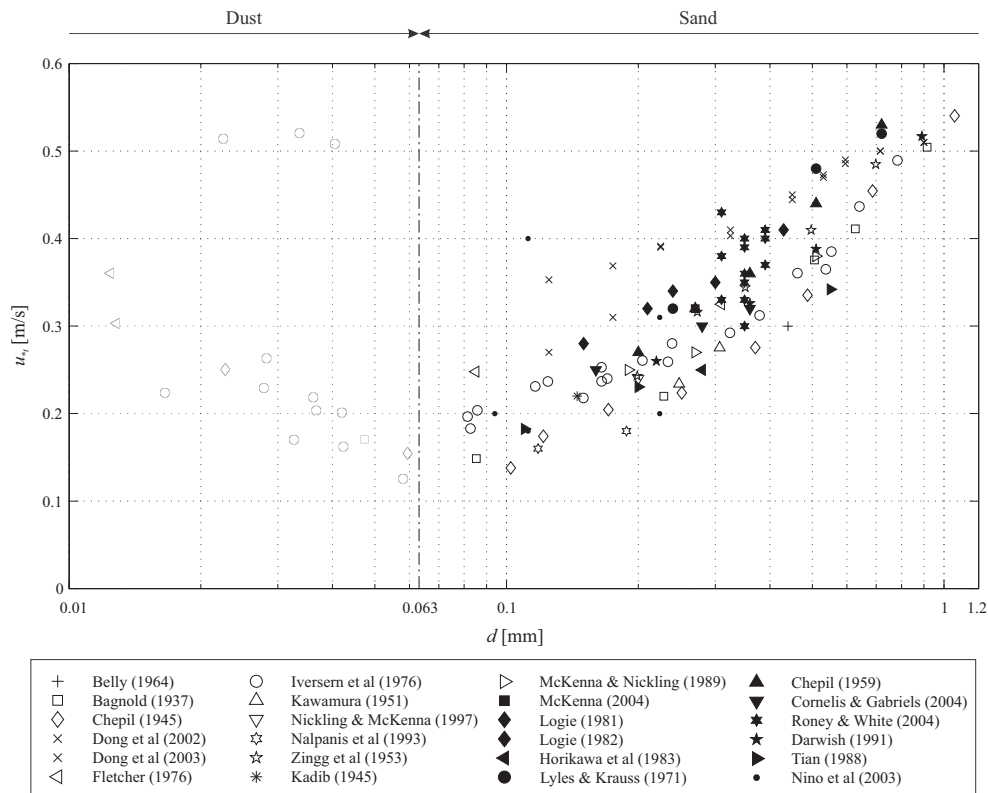


Fig. 2. Threshold shear velocity measurements collected in literature: dust (empty light grey markers) and sand.

originally adopted by the authors of the models. The models by Bagnold (1941) (Eq. (1)) and Shao and Lu (2000) (Eq. (2)) are selected because of their compactness, i.e. their dependence from a small number of empirical parameters (A_b , A_s and γ). The two semi-empirical models are

$$u_{*t} = A_b \sqrt{\frac{\rho_p - \rho_a}{\rho_a} g d}, \quad (1)$$

$$u_{*t} = A_s \sqrt{\frac{\rho_p - \rho_a}{\rho_a} g d + \frac{\gamma}{\rho_a d}}. \quad (2)$$

where ρ_p and ρ_a are particle and air density, respectively, and g is gravitational acceleration. Beside the single-valued estimates of a goodness-of-fit, for each model the prediction Confidence Intervals (CIs) are evaluated at 5th and 95th percentiles, i.e. the interval within which the true mean value is expected to lie. Fig. 3 compares the refitted laws to the original ones, while the corresponding model parameters are summarized in Table 2. The following remarks can be outlined:

- for both fittings $R^2 \approx 0.75$. On the one hand, this relatively high value confirms grain size is the primary control of u_{*t} . On the other hand, the value is by far lower than unit: hence, u_{*t} cannot be approximated as a deterministic function of d . In other words, the deterministic approach is not able to completely capture the threshold variability.
- both refitted laws pretty agree for $d > 0.2$ mm, i.e. they share both the asymptotic trend due to the common dependency of u_{*t} on \sqrt{d} , and the intercept, i.e. $A_b = 0.127 \approx A_s = 0.124$. This

finding is in the spirit of the Shao's model, whose corrective term $\gamma/\rho_a d$ is conceived to modify Bagnold's model at low d only;

- generally speaking, the refitted laws predict higher values of u_{*t} for given d . It is worth pointing out that the ensemble includes a number of poorly sorted and natural sands, while the ensemble originally adopted by Bagnold (1941) and Shao and Lu (2000) were limited to sand as uniform as possible. Hence, interspersed small particles provide additional cohesive forces also for medium and coarse natural sands (Roney and White, 2004);
- Regarding the model by Shao and Lu (2000) at small d , the refitted law predicts u_{*t} values lower than the original law, because fitting is restricted to sands and exclude dusts. In other words, the refitted Shao's law mimics herein only the sand physics, and its trend at low d is not driven by the dust physics, and notably by the very high values $u_{*t} \approx 0.5$ m/s provided by Iversen et al. (1976) at $d = 0.023, 0.034, 0.041$ mm and $u_{*t} > 1$ m/s provided by Fletcher (1976) at $d = 0.008, 0.009$ mm. A lower value of γ for the refitted law follows;
- CI of the Bagnold fitting is quite narrow (being the model easily reducible to a linear regression model). Conversely, the lower d is, the wider CI in Shao's model is, because of the statistical uncertainty on the parameter γ (Eq. 2), which has its main effects for small d .

4. Statistical approach: copula-based quantile regression

In the following a statistical approach is proposed, having in mind both the number of uncertainty sources and the limitations of the deterministic approach.

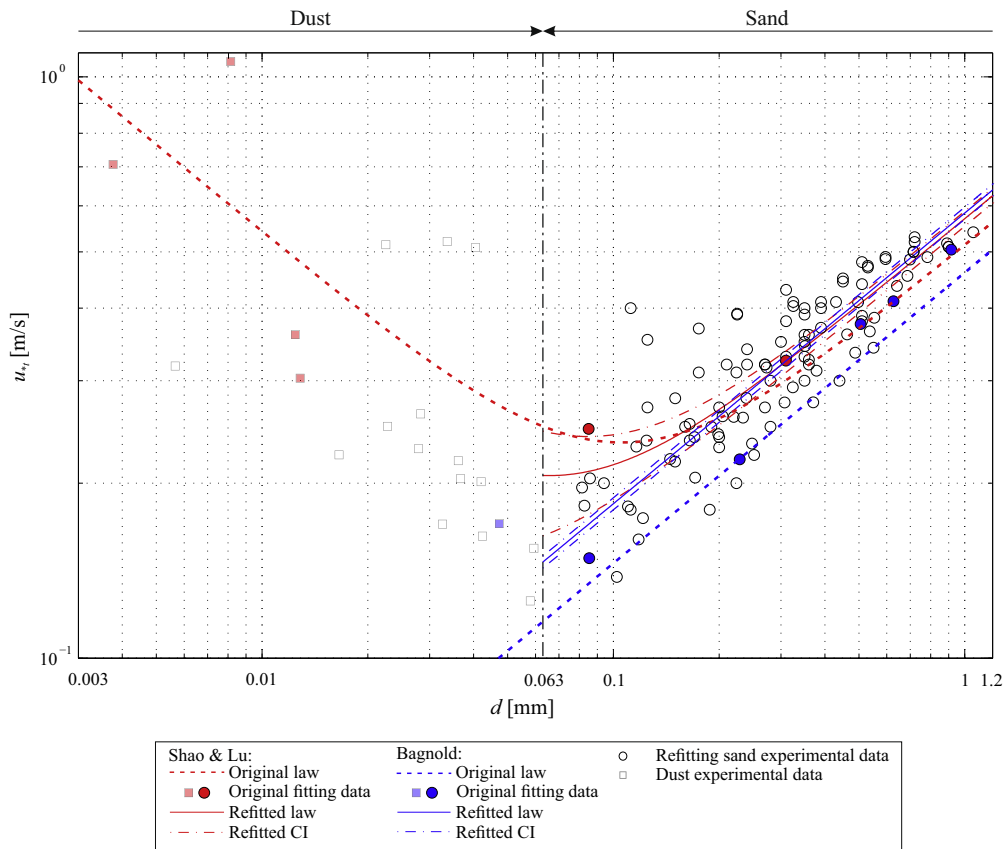


Fig. 3. Non-linear regression and CIs for Bagnold (1941) and Shao and Lu (2000)

Table 2
Original and refitted model parameters

	Original parameters		Refitted parameters	
	Bagnold (1941)	Shao and Lu (2000)	Bagnold (1941)	Shao and Lu (2000)
A [-]	0.100	0.111	0.127	0.124
γ [N/m]	–	2.9×10^{-4}	–	1.12×10^{-4}
R^2	–	–	0.74	0.75

Each source of uncertainty and related microscopic parent r.v. are not separately described in statistical terms. Conversely, the threshold shear velocity is modeled as a single, comprehensive, bulk random variable that reflects the effects of all the sources of uncertainty. A continuous dependence of such a random variable on the reference diameter is clearly observed in terms of mean by the deterministic approach. The adopted statistical method is intended to:

- recognize and describe, if any, the dependence of u_{*t} on d not only in terms of mean value but also with reference to higher statistical moments and percentiles;
- discard bias eventually due to the relatively low cardinality of the learning data set and to the non uniform distribution of the reference diameters within it. In fact, the reference diameter that happened to be employed in each original study is not a random variable but a deterministic setup feature. However, the ensemble of sand diameters tested in existing literature does not result from a deterministic research plan.

In order to reach the goals above, it is useful to consider the ensemble of the reference diameter collected from literature as a set of realizations of a random variable. This allows to quantitatively describe in proper statistical terms the structure of dependence between the random variable of interest u_{*t} and the sand diameter d by means of the copula modelling. In conceptual terms, the copula modelling allows to express the dependence of two random variables (e.g. u_{*t} and d in this case) through subdivision of their joint distribution into two contributions: the marginal distributions of the individual r.v.s and their interdependency, described by the copula (Venter, 2002). From the joint distribution, one can derive the distributions of u_{*t} conditioned to given values of d , and any corresponding percentiles of interests.

4.1. Adopted method

In the following the copula modelling is briefly outlined, having in mind that only recently it has been introduced in some engineering fields (see e.g. Genest and Favre, 2007 in hydrology) and physical sciences (see e.g. Schölzel and Friederichs, 2008 in geophysics). For the sake of generality, in this Section the r.v.s of our interest, d and u_{*t} , are replaced by two general r.v.s, X and Y , respectively. Given the joint cumulative distribution function $F(x, y)$ of a pair of random variables (X, Y) , under suitable assumptions of continuity (Nelsen, 2007), it can be also written as

$$F(x, y) = C\{F_X(x), F_Y(y)\}, \quad x, y \in \mathbb{R} \quad (3)$$

where F_X and F_Y are the cumulative marginal distributions of X and Y , respectively, while $C: [0, 1]^2 \rightarrow [0, 1]$ is the copula of the pair (X, Y) .

The copula C , which is the cumulative joint distribution of a pair (U, V) of variables uniformly distributed over $[0, 1]$, entirely expresses the dependence structure between X and Y , removing the effects of marginal distributions, and letting immediately observable its main characteristic, like, e.g., positive or negative concordance. Using copulas in estimation of joint distributions,

or estimation of relationships among random variables, marginal distributions are firstly evaluated and then a specific copula is fitted with respect to the empirical one available by experimental measurements, i.e. the learning data set. Having removed the effect of marginal behaviours, the copula selection is independent of the marginal distribution choice (Trivedi and Zimmer, 2005). Several copulas are reported in literature (Nelsen, 2007). For instance, inverted Clayton copula, also known as Heavy Right Tail copula or Burr copula (see, e.g. Venter, 2002; de Waal and van Gelder, 2005), is reported below being the employed copula in Section 4.2.2.

$$C(u, v) = u + v - 1 + \left[(1-u)^{-1/\alpha} + (1-v)^{-1/\alpha} - 1 \right]^{-\alpha}, \quad u, v \in [0, 1], \alpha > 0 \quad (4)$$

where α is a fitting parameter. Once the copula is fitted according to available measurements, a sample of any cardinality can be generated. Thus, $C(u, v)$ can be transformed back into the original units using the marginal distributions. In fact, the resulting pairs $(x, y) = (F_X^{-1}(u), F_Y^{-1}(v))$ can be deduced by inverting the cumulative distribution functions (see Genest and Favre, 2007 for further details). From the copula generated sample one can derive conditional probability density functions of Y given X . In turn, point wise percentiles $p_\tau(y)$ of Y can be deduced from the conditional probability density functions. In fact, given the joint cumulative distribution function $F(x, y)$, it can be first derived the joint density (Eq. 5) and the conditional density (Eq. 5) and

$$f(x, y) = \frac{\partial^2 F(x, y)}{\partial x \partial y} \quad (5)$$

$$f(y|x) = \frac{f(x, y)}{f_X(x)} \quad (6)$$

from which, any percentile can be obtained as

$$p_\tau(y) = Q_{Y|X}(\tau) \quad (7)$$

where $Q_{Y|X}(\tau)$ is the τ th quantile of Y given X . Alternatively, the copula modelling allows to directly evaluate high order statistics and perform a quantile regression to obtain any percentile of Y as a function of X . From Bouyé and Salmon (2009), fixing the conditional probability of Y given $X=x$ at some quantile τ , so that $\partial C(u, v)/\partial u = \tau$, and solving for v , we have (Koenker, 2005):

$$p_\tau(v) = Q_{V|U}(\tau|u) \quad (8)$$

and consequently,

$$p_\tau(y) = F_Y^{-1}(Q_{V|F(X)}(\tau|F(x))) \quad (9)$$

is defined the quantile regression function conditional on X . Hence, in function of τ , one can define any quantile curve of the random variable Y .

4.2. Results

In the following the results are presented and discussed by retracing the main methodological steps previously outlined. In

Section 4.2.1, the marginal distributions $F(d)$ and $F(u_{*t})$ are fitted. In Section 4.2.2, a specific copula is fitted with respect to the learning data set. Finally in Section 4.2.3, the bivariate joint density $f(d, u_{*t})$ is recovered and the conditional probability density functions $f(u_{*t}|d)$ are obtained.

4.2.1. Fitting the marginal distributions

Since the marginal distributions of $F(d)$ and $F(u_{*t})$ are a priori unknown, we first aim at assessing which distributions for the diameter and for the threshold shear velocity fit the collected data set. Several guess parametric distributions are considered, such as lognormal, loglogistic, gamma, Weibull. In order to assess the goodness of the fit, Anderson and Darling (1952) test is used because of the high weight placed on observations in the tails of distribution. The null hypothesis is not rejected for any tested parametric distribution, being the resulting p -values always greater than its threshold value $p_t = 0.05$. Among tested parametric distributions, lognormal and gamma ones resulted in the highest p -values. In particular, lognormal distribution is highly scored ($p \approx 0.87$) for d , while for u_{*t} the gamma distribution obtains the largest p -value ($p \approx 0.71$). Fig. 4 collects the empirical cumulative distributions functions and the best fitting parametric ones (lognormal and gamma). For the sake of generality, also non-parametric distributions based on kernel method are considered. Gaussian kernels are adopted. Their supports are bounded to positive values having in mind the physical meaning of the r.v.s. In particular, the lower bound of d is not forced to be equal to the conventional limit diameter between dust and sand. Indeed, this deterministic nominal value does not comply with the adopted statistical approach. The kernel cumulative distributions functions for d and u_{*t} are also plotted in Fig. 4. Both parametric and non parametric distributions fit well the empirical one at the lower tail but depart at the upper tail, probably not resolved enough by the available data. The kernel distribution s best fit around the median values of d and u_{*t} . In the following the non parametric distribution is retained for the sake of generality and because of its goodness-of-fit.

4.2.2. Copula fitting

The original learning data set is plotted in terms of d - u_{*t} pairs in Fig. 5-a, -a, together with the empirical and non parametric marginal distributions. Hence, it is reduced to the copula scale and shown in terms of scatter plot of the $F(d)$ - $F(u_{*t})$ pairs in Fig. 5(b). From Fig. 5(b) one can observe that the transformed learning data set is strongly correlated with only upper tail dependence. In other words, the points are concentrated in the upper right corner and

they open approaching the lower left corner. This empirical qualitative evidence drives the choice of the copula family to be adopted for fitting (Schölzel and Friederichs, 2008; Genest and Favre, 2007). On the one hand, elliptical copulas, i.e. Gaussian or Student-t copula, are expected to be inappropriate to describe such a dependence because of their symmetric tail behaviour. On the other hand, Archimedean copulas, e.g. Frank, or Clayton copula, being in principle asymmetric, allow for simulating different tail behaviour. Because of their flexibility, Archimedean copulas have been previously applied to others physical problems such as in geoscience (Schölzel and Friederichs, 2008). For real world, low-cardinality learning data set the choice of the copula can be performed a posteriori by comparing the $F(d)$ - $F(u_{*t})$ scatter plot of the observed data set to an artificial data set generated from the fitted copula (Genest and Nešlehová, 2014). Such graphical diagnostics of goodness-of-fit is performed for several guess copulas. The cardinality of the artificial data is set equal to $\# = 2000$ for the sake of clarity in visualization. Results about the copulas not further retained are shown in Fig. 6, while the inverted Clayton best fitting copula is assessed in Fig. 5(c). Observed data set is highlighted using black marks, while grey marks are used for the artificial data set. Elliptical copulas (t-student and Gaussian ones, Fig. 6-a, -b, -a, -b, respectively) predict high and equal dependence at both upper tail, i.e. close to (1, 1), and lower tail, i.e. around (0, 0), in line with the theory. Frank copula (Fig. 6-c) shows no tail dependencies and Clayton copula (Fig. 6-d) shows lower tail dependence only: both are not suited to replicate the observed dependence. Conversely, the inverted Clayton copula (Fig. 5-c) replicates the heavy concentration of probability in the upper tail, and lower dependence in the lower tail. Only a light discrepancy can be observed by the fact that the scatter plot of learning data set is slightly asymmetric with respect to the bisector, while the inverted Clayton copula is not. The inverted Clayton best fit results in copula parameter $\alpha = 3.7$ and Kendall's rank correlation $\tau = 0.65$. The convergence of the copula parameter α is checked for increasing number n of the learning data included in the set, being $n \leq 109$. α itself as well as its weighted residual error $\alpha_{res,n} = |(\alpha_n - \alpha_{n-1})/\alpha_n|$ are evaluated for growing sizes n and averaged over 1000 random permutation of the order of the learning data set. The convergences versus n are plotted in Fig. 7. The convergence of α (Fig. 7-a) shows an overall monotonic trend and the convergence rate at complete learning data set ($n = \# = 109$) is very low. The weighted residual error $\alpha_{res,n} \approx 10^{-3}$ at $n = \# = 109$ is low enough for practical applications (Fig. 7-b). In spite of such an encouraging overall convergence, higher accuracy would need higher cardinality of the learning data set. Finally, in Fig. 5(d),

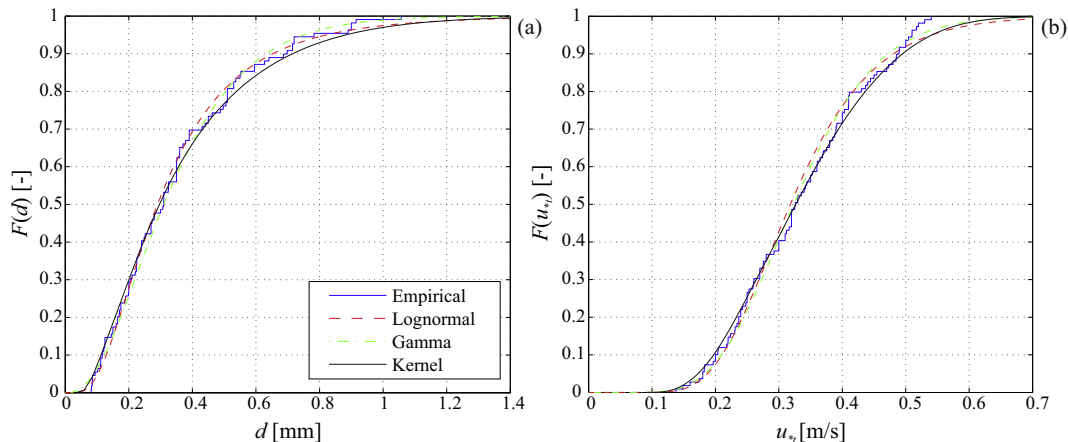


Fig. 4. Marginal distributions fitting: sand diameter (a) and threshold shear velocity (b)

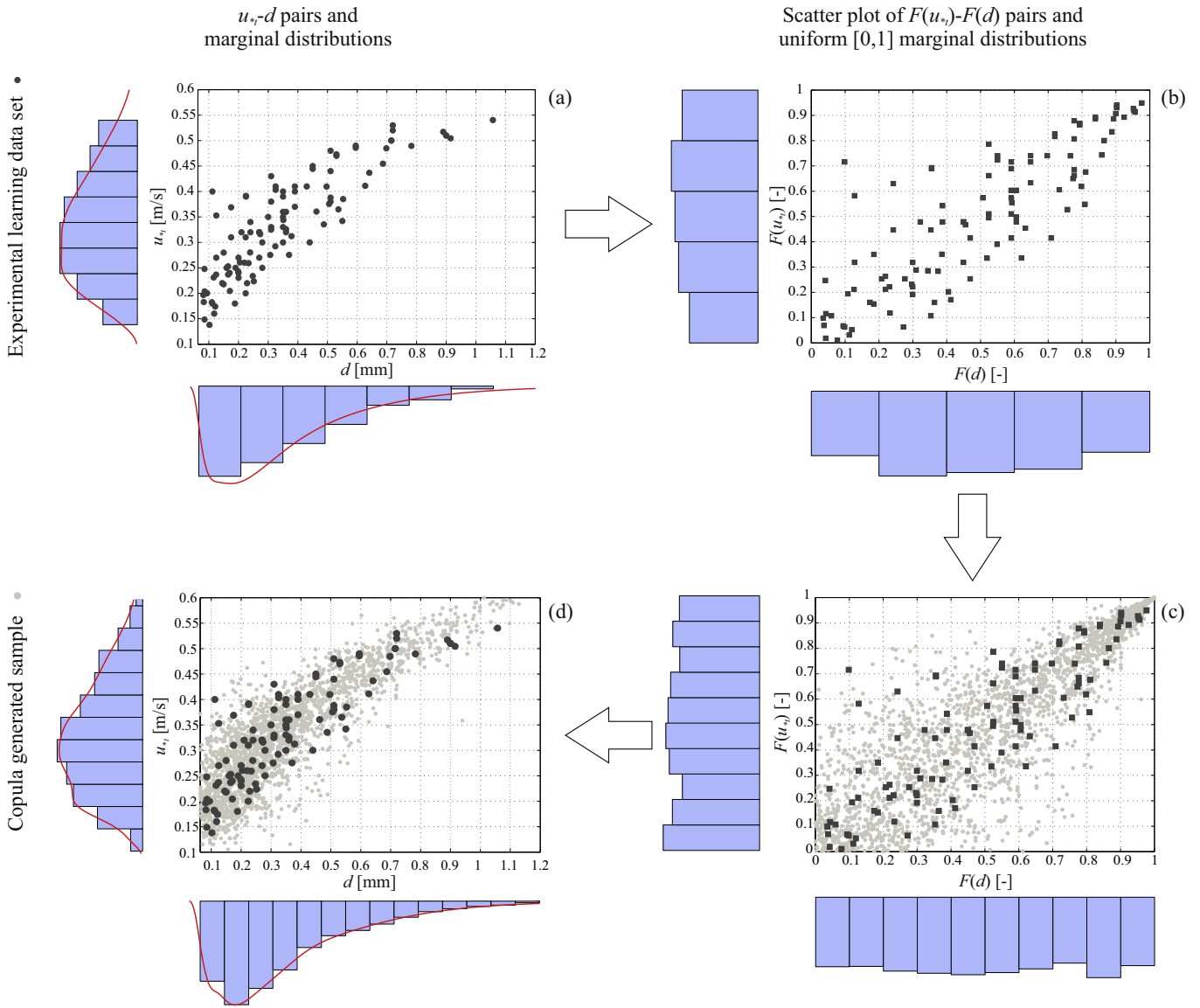


Fig. 5. Copula fitting to experimental learning data set: plot of experimental learning data set (a), scatter plot of the pairs $F(d)$ and $F(u_{*t})$ (b), random sample from inverted Clayton copula (c), resizing to original scale of the learning data set (d).

the pairs $F(d) - F(u_{*t})$ are resized back to the original scale of the data calculating the inverted kernel cumulative distribution. The corresponding marginal distributions are plotted in the same Figure. Both $d - u_{*t}$ pairs and marginal distributions well agree with the ones related to the observed original data.

4.2.3. Joint and conditional distributions

In the following the cardinality of the artificial sample is increased from $\# = 2.000$ to $\# = 10.000.000$ in order to further proceed in the post processing of the joint and conditional probability density functions. The joint probability density function $f(d, u_{*t})$ of the two random variables d and u_{*t} is recovered by evaluating expression (5). It is plotted in Fig. 8, where the learning data set is superimposed. Hence, the conditional probability density functions of the threshold shear velocity $f(u_{*t}|d)$ for given values of the diameter d are obtained according to Eq. (6). In Fig. 9(a), several $f(u_{*t}|d)$ are plotted for some selected values of d in the range $0.063 \leq d \leq 1.2$. The coefficient of variation *c.o.v.* and the skewness *sk* of the conditional probability density functions are plotted

versus the diameter in Figs. 9(a) and (b). The following remarks can be outlined:

- the higher the diameter is, the higher the mean value of the threshold shear velocity and the lower its variance are;
- the monotonic decrease of the coefficient of variation for growing reference diameter properly reflects the expected decreasing role played by interparticle forces and related uncertainties. The coefficient of variation attains values in the range $0.05 \leq c.o.v. \leq 0.25$, i.e. moderate but not negligible values with respect to other in situ environmental r.v.s (e.g. turbulent wind velocity). We conjecture this is due to the fact that wind tunnel setup conditions are more controlled than in situ ones;
- the skewness values indicate that the conditional probability functions are not fully symmetric, except around $d \approx 0.22\text{mm}$ where $sk \approx 0$. Skewness is weakly positive (up to $sk = 0.6$) for fine sands ($0.063 \leq d < 0.22\text{mm}$), that is the probability density function is right tailed or, in other terms, not negligible probability density occurs at u_{*t} values quite higher than the mode.

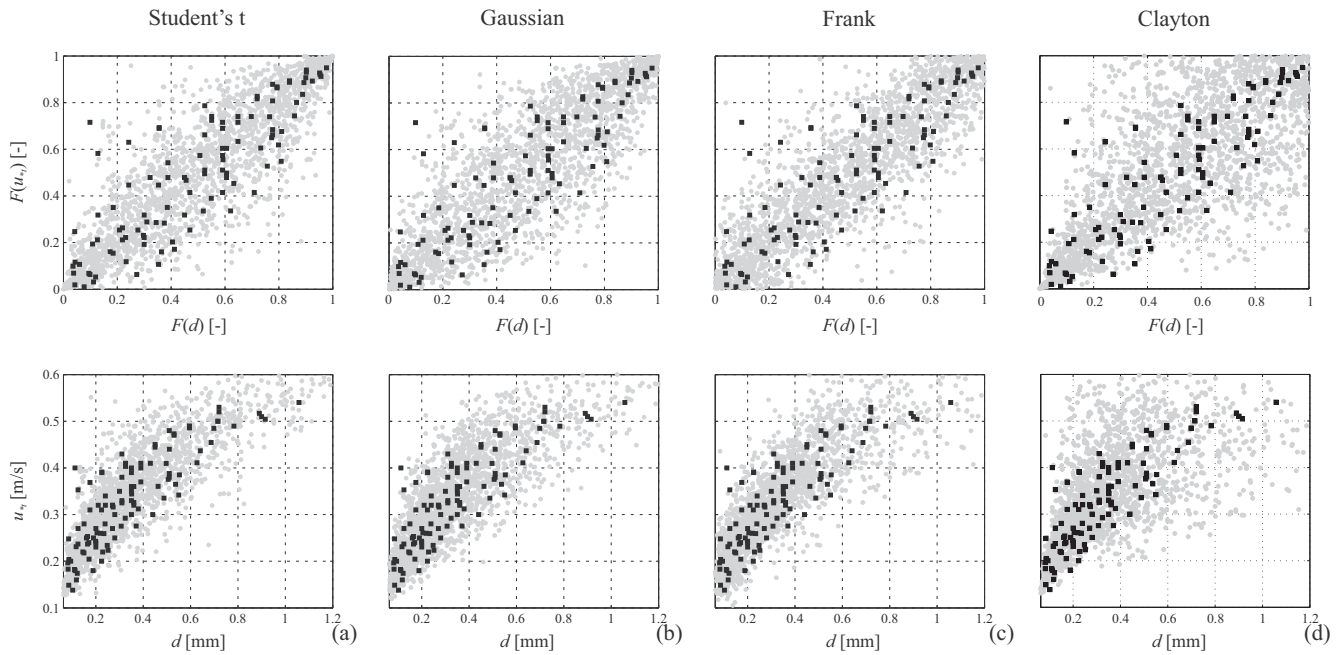


Fig. 6. Graphical diagnostics of goodness-of-fit for not retained copulas.

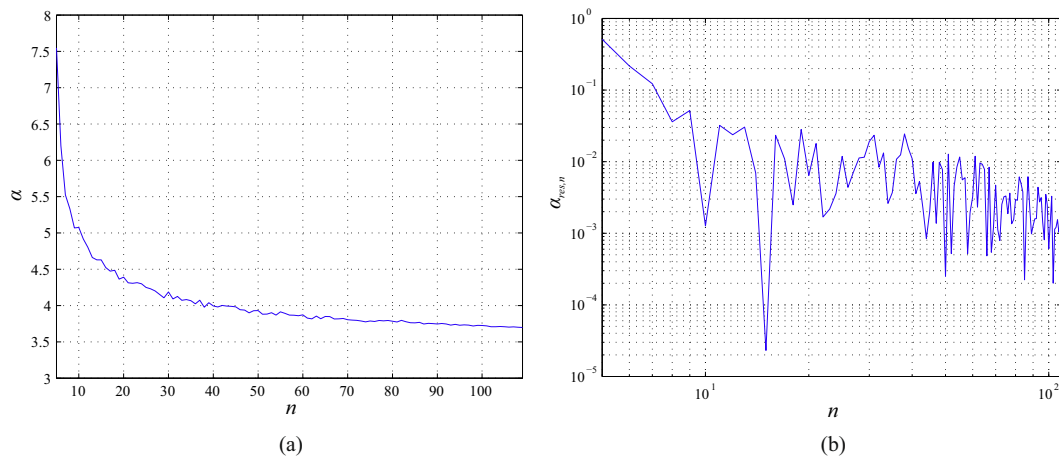


Fig. 7. Convergence of copula fitting in terms of the parameter α (a) and weighted residual $\alpha_{res,n}$ (b).

The Authors conjecture that cohesive resisting force is the main physical cause of such positive skewness. Conversely, skewness is moderately negative (up to $sk \approx -1$) for medium and coarse sands ($0.22 < d \leq 1.2\text{mm}$). In such an interval, sk trend versus d is no longer monotonic and increases for diameters higher than about 0.7mm (coarse sand). The Authors conjecture that Saffman lift force is the main physical cause of such negative skewness (Saffman, 1965). In turn, the lift force is expected to be affected by the uncertain grain relative position with respect to other bed particles.

Any other statistical moment or percentiles can be evaluated for each conditional probability functions. For instance, Fig. 9(d) plots the 5th percentile - mean value ratio versus the sand diameter. The quasi-monotonically increasing trend is qualitatively opposite to the decreasing of $c.o.v.$. The values vary in the range $0.6 \leq p_5/\mu \leq 0.94$, i.e. the 5th percentile is around 0.65 times the mean value for fine sands and it reaches almost 0.94 times the mean value for coarse sands.

5. Comparison between deterministic and statistical approach

Finally, the main findings of the proposed statistical approach are critically compared to the results of the deterministic approach. Fig. 10 collects the original learning data set, the refitted deterministic laws of $u_{*t}(d)$ and some statistics obtained from the conditional probability density distributions $f(u_{*t}|d)$: the mean value $\mu(u_{*t})$, the 1st, 5th, 25th, 75th, 95th and 99th percentiles.

It is worth pointing out that:

- the mean value $\mu(u_{*t})$ overall agrees with the refitted law proposed by Shao and Lu (2000), even if they result from completely different approaches. Generally speaking, the statistical approach provides consistent results in mean terms with the traditional and most established deterministic laws: this outcome is expected because of the common learning data set, but is not for granted;
- in addition, the proposed statistical approach enriches substantially the description of u_{*t} versus d . Indeed, for a given diameter

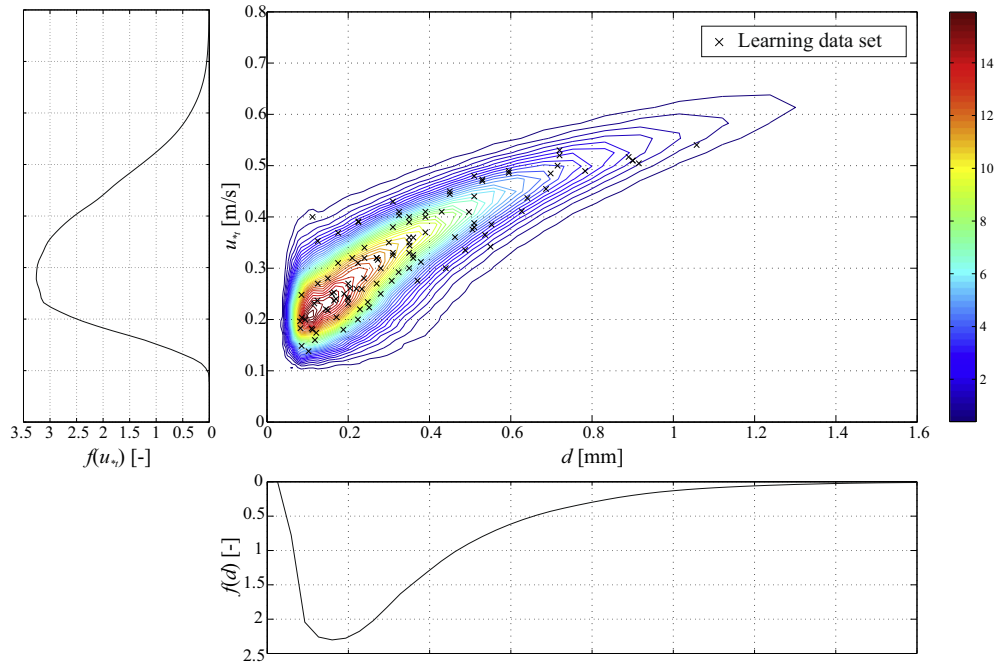


Fig. 8. Joint and marginal probability density functions derived from copula fitting.

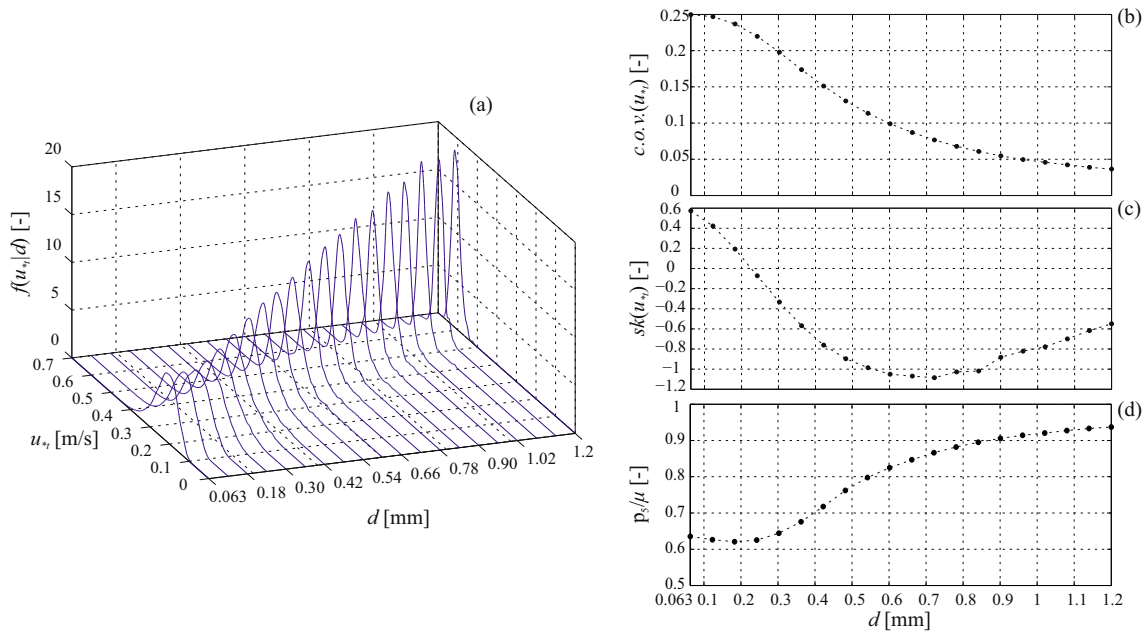


Fig. 9. Conditional distributions of u_{*t} on d (a), coefficient of variation (b), skewness (c) and 5th percentile – mean value ratio (d) of u_{*t} as a function of d .

any value of the threshold shear velocity is associated to a probability of not-exceedance;

- in lieu of adopting the nominal value of u_{*t} , a given safety level can be set in engineering practice, and the corresponding value of the threshold shear velocity adopted in the estimation of the sand transport rate.

6. Conclusions

The present study critically compares deterministic and statistical approaches to threshold shear velocity on the basis of the

collection of a huge amount of experimental measurements. Since the description of each random variable affecting u_{*t} is hard to be practically tractable, each source of uncertainty (aleatory and epistemic) is merged within the bulk random variables u_{*t} . The present study does not aim at ascertaining which source of uncertainty among aleatory and epistemic ones mostly affects the variability of the fluid threshold velocity, and the proposed statistical approach is not able to deal with this goal. In the case epistemic uncertainties are predominantly responsible for the overall uncertainties, recently proposed generalized approaches for uncertainty quantification would be more suitable (Beer and Ferson, 2013; Beer and Patelli, 2015 and references therein).

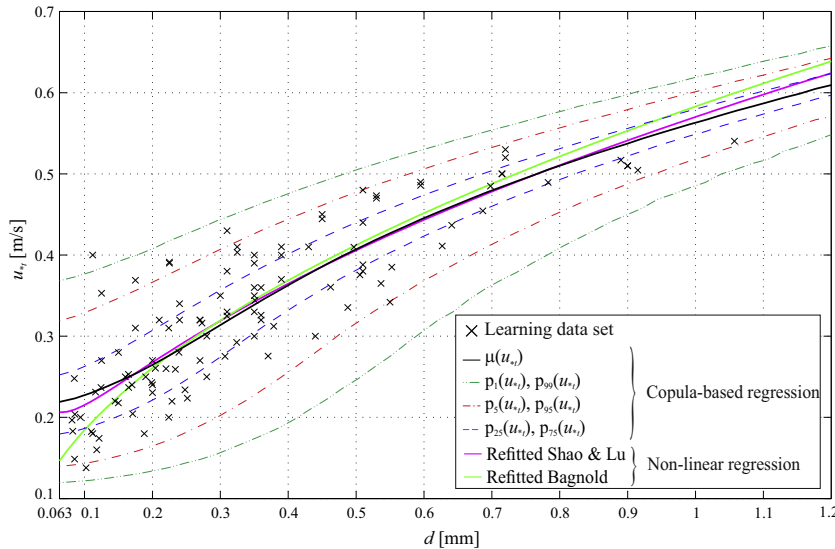


Fig. 10. Comparison between copula regression and non-linear regression: mean values $\mu(u_{*t})$, $p_1(u_{*t})$, $p_5(u_{*t})$, $p_{25}(u_{*t})$, $p_{75}(u_{*t})$, $p_{95}(u_{*t})$, $p_{99}(u_{*t})$ percentiles versus refined Bagnold (1941) and Shao and Lu (2000) laws.

The deterministic approach is updated thanks to the amount of collected data: in spite of a satisfying fitting of the $u_{*t}(d)$ nominal law, the lack of information about u_{*t} variability remains a shortcoming of the approach.

The proposed statistical approach allows to enrich the threshold shear velocity description providing measures of its variance and high order statistics, notably extreme percentiles. The proper definition of u_{*t} values associated with given not-exceedance probabilities allows to predict aeolian events magnitude in probabilistic terms and to assess related risk in a number of fields of application, such as geomorphology, environmental protection or infrastructure engineering.

In the light of the obtained results, we suggest two research perspectives. First, a high cardinality of the dataset would allow a better copula fitting: the authors hope that further independent experimental studies will enrich the learning data set. Second, it would be worth investigating the uncertainty propagation from threshold shear velocity to sand transport rate.

Acknowledgments

The study has been developed in the framework of the Wind-blown Sand Modelling and Mitigation joint research, development and consulting group established between Politecnico di Torino and Optiflow Company. The authors wish to thank Davide Fransos, member of the WSM group, for the helpful discussions about the topics of the paper. The research that led to the present paper was partially supported by a Grant of the group GNFM of INdAM.

References

- Alghamdi, A.A., Al-Kahtani, N.S., 2005. Sand control measures and sand drift fences. *J. Perform. Constr. Facil.* 19, 295–299. [http://dx.doi.org/10.1061/\(ASCE\)0887-3828\(2005\)19:4\(295\)](http://dx.doi.org/10.1061/(ASCE)0887-3828(2005)19:4(295)).
- Anderson, T., Darling, D., 1952. Asymptotic theory of certain goodness of fit criteria based on stochastic processes. *Ann. Math. Stat.* 23, 193–212.
- Andreotti, B., 2004. A two-species model of aeolian sand transport. *J. Fluid Mech.* 510, 47–70. <http://dx.doi.org/10.1017/S0022112004009073>.
- Bagnold, R., 1941. The physics of blown sand and desert dunes. Methuen. <http://dx.doi.org/10.1007/978-94-009-5682-7>.
- Bagnold, R.A., 1937. The transport of sand by wind. *Geogr. J.* 89, 409–438. <http://dx.doi.org/10.2307/1786411>.
- Barchyn, T.E., Hugenholtz, C.H., 2011. Comparison of four methods to calculate aeolian sediment transport threshold from field data: Implications for transport

- prediction and discussion of method evolution. *Geomorphology* 129, 190–203. <http://dx.doi.org/10.1016/j.geomorph.2011.01.022>.
- Beer, M., Ferson, S., 2013. Special issue of mechanical systems and signal processing imprecise probabilities – what can they add to engineering analyses? *Mech. Syst. Signal Process.* 37, 1–3.
- Beer, M., Patelli, E., 2015. Editorial: engineering analysis with vague and imprecise information. *Struct. Saf. Part B* 143.
- Belly, P.Y., 1964. Sand movement by wind. Technical Report 1. U.S. Army - Corps of Engineers. US Army Coastal Eng. Res. Center, Washington, DC.
- Blott, S., Pye, K., 2006. Particle size distribution analysis of sand-sized particles by laser diffraction: an experimental investigation of instrument sensitivity and the effects of particle shape. *Sedimentology* 53, 671–685. <http://dx.doi.org/10.1111/j.1365-3091.2006.00786.x>.
- Bouyé, E., Salmon, M., 2009. Dynamic copula quantile regressions and tail area dynamic dependence in forex markets. *Eur. J. Finance* 15, 721–750. <http://dx.doi.org/10.1080/13518470902853491>.
- Burr, D., Bridges, N., Marshall, J., Smith, J., White, B., Emery, J., 2015. Higher-than-predicted saltation threshold wind speeds on titan. *Nature*, 517.
- Cheng, J., Xue, C., 2014. The sand-damage prevention engineering system for the railway in the desert region of the qinghai-tibet plateau. *J. Wind Eng. Ind. Aerodyn.* 125, 30–37. <http://dx.doi.org/10.1016/j.jweia.2013.11.016>.
- Chepil, W., 1945. Dynamics of wind erosion: II. initiation of soil movement. *Soil Sci.* 60, 397–411. <http://dx.doi.org/10.1097/00010694-194511000-00005>.
- Chepil, W., 1959. Equilibrium of soil grains at threshold of movement by wind. *Soil Sci. Soc. Proc.* 23, 422–428.
- Chepil, W.S., 1951. Properties of soil which influence wind erosion: IV. State of dry aggregate structure. *Soil Sci.* 72, 387–401.
- Claudin, P., Andreotti, B., 2006. A scaling law for aeolian dunes on mars, venus, earth, and for subaqueous ripples. *Earth Planet. Sci. Lett.* 252, 30–44.
- Cornelis, W., Gabriels, D., 2004. A simple model for the prediction of the deflation threshold shear velocity of dry loose particles. *Sedimentology* 51, 39–51.
- Darwish, M., 1991. Threshold friction velocity: moisture and particle size effect (Master's thesis). Texas Tech University.
- Dong, Z., Liu, X., Wang, H., Wang, X., 2003. Aeolian sand transport: a wind tunnel model. *Sediment. Geol.* 161, 71–83. [http://dx.doi.org/10.1016/S0037-0738\(02\)00396-2](http://dx.doi.org/10.1016/S0037-0738(02)00396-2).
- Dong, Z., Liu, X., Wang, H., Zhao, A., Wang, X., 2002. The flux profile of a blowing sand cloud: a wind tunnel investigation. *Geomorphology* 49, 219–230. [http://dx.doi.org/10.1016/S0169-555X\(02\)00170-8](http://dx.doi.org/10.1016/S0169-555X(02)00170-8).
- Duan, S.Z., Cheng, N., Xie, L., 2013. A new statistical model for threshold friction velocity of sand particle motion. *Catena* 104, 32–38. <http://dx.doi.org/10.1016/j.catena.2012.04.009>.
- Edwards, B., Namikas, S., 2015. Characterizing the sediment bed in terms of resistance to motion: toward an improved model of saltation thresholds for aeolian transport. *Aeolian Res.* 19, 123–128. <http://dx.doi.org/10.1016/j.aeolia.2015.10.004>.
- Fletcher, B., 1976. Incipient motion of granular materials. *J. Phys. D Appl. Phys.* 9, 2471–2478. <http://dx.doi.org/10.1088/0022-3727/9/17/007>.
- Foley, A., 2010. Uncertainty in regional climate modelling: a review. *Prog. Phys. Geogr.* 34, 647–670.
- Friedman, G., Sanders, F., 1978. *Principles of Sedimentology*. Wiley, New York.
- Genest, C., Favre, A.C., 2007. Everything you always wanted to know about copula modeling but were afraid to ask. *J. Hydrol. Eng. (ASCE)* 12, 347–368. [http://dx.doi.org/10.1061/\(ASCE\)1084-0699\(2007\)12:4\(347\)](http://dx.doi.org/10.1061/(ASCE)1084-0699(2007)12:4(347)).

- Genest, C., Nešlehová, J., 2014. Copulas and copula models. Wiley StatsRef: Statistics Reference Online. John Wiley & Sons, Ltd. <http://dx.doi.org/10.1002/9781118445112.stat07523>.
- Gillette, D.A., Marticorena, B., Bergametti, G., 1998. Change in aerodynamic roughness height by saltating grains: experimental assessment, test of theory, and operational parameterization. *J. Geophys. Res.* 103, 6203–6209.
- Greeley, R., Iversen, J.D., 1985. Wind as a Geological Process on Earth, Mars, Venus, and Titan. Cambridge University Press, New York. <http://dx.doi.org/10.1017/CBO9780511573071>.
- Greeley, R., Leach, R., White, B., Iversen, J., Pollack, J., 1976. Mars – wind friction speeds for particle movement. *Geophys. Res. Lett.* 3, 417–420.
- Halpern, J.Y., 2003. Reasoning About Uncertainty. MIT Press.
- Horikawa, K., Hotta, S., Kubota, S., Katori, S., 1983. On the sand transport rate by wind on a beach. *Coastal Eng. Japan* 26, 101–120.
- ISO14688-1:2002, Geotechnical investigation and testing – identification and classification of soil – part 1: Identification and description.
- Iversen, J.D., Pollack, J.B., Greeley, R., White, B.R., 1976. Saltation threshold on mars: the effect of interparticle force, surface roughness, and low atmospheric density. *Icarus* 29, 381–393. [http://dx.doi.org/10.1016/0019-1035\(76\)90140-8](http://dx.doi.org/10.1016/0019-1035(76)90140-8).
- Iversen, J.D., White, B.R., 1982. Saltation threshold on earth, mars and venus. *Sedimentology* 29, 111–119. <http://dx.doi.org/10.1111/j.1365-3091.1982.tb01713.x>.
- Jones, R., Pollock, H., Cleaver, J., Hodges, C., 2002. Adhesion forces between glass and silicon surfaces in air studied by afm: effects of relative humidity, particle size, roughness and surface treatment. *Langmuir* 18, 8045–8055. <http://dx.doi.org/10.1021/la0259196>.
- Kadib, A.L., 1964. Sand transport by wind – Addendum II to sand movement by wind. Technical Report 1. U.S. Army – Corps of Engineers. US Army Coastal Eng. Res. Center, Washington, DC.
- Kawamura, R., 1951. Study of sand movement by wind. Technical Report. Translated (1965) as University of California Hydraulics Engineering Laboratory Report HEL 2–8. Berkeley.
- Koenker, R., 2005. Quantile Regression. Cambridge University Press.
- Kok, J.F., 2010. Analytical calculation of the minimum wind speed required to sustain wind-blown sand on earth and mars. ArXiv e-prints. <http://arxiv.org/ftp/arxiv/papers/1001/1001.4840.pdf>.
- Kok, J.F., Parteli, E.J.R., Michaels, T.I., Karam, D.B., 2012. The physics of wind-blown sand and dust. *Prog. Phys. Rep.* doi:<http://dx.doi.org/10.1088/0034-4885/75/10/106901>.
- Lancaster, N., Nickling, W.G., 1994. Geomorphology of Desert Environments. Springer, Netherlands. chapter Aeolian sediment transport.
- Li, B., Ellis, J., Sherman, D., 2014. Estimating the impact threshold for wind-blown sand. *J. Coastal Res.* 70, 627–632.
- Logie, M., 1981. Wind tunnel experiments on dune sands. *Earth Surf. Proc. Land* 6, 365–374.
- Logie, M., 1982. Influence of roughness elements and soil moisture on the resistance of sand to wind erosion. *Catena Suppl.* 1, 161–174.
- Lyles, L., Krauss, R., 1971. Threshold velocities and initial particle motion as influenced by air turbulence. *Trans. ASAE*, 14563–14566.
- McEwan, I., Heald, J., 2001. Discrete particle modeling of entrainment from flat uniformly sized sediment beds. *J. Hydraulic Eng.* 127, 588–597.
- McKenna, N.C., 2003. Effects of temperature and humidity upon the entrainment of sedimentary particles by wind. *Boundary Layer Meteorol.* 108, 61–89. <http://dx.doi.org/10.1023/A:1023035201953>.
- McKenna Neuman, C., 2004. Effects of temperature and humidity upon the transport of sedimentary particles by wind. *Sedimentology* 51, 1–17.
- McKenna Neuman, C., Nickling, W., 1989. A theoretical and wind tunnel investigation of the effect of capillary water on the entrainment of sediment by wind. *Can. J. Soil Sci.* 69, 79–96.
- Merrison, J., 2012. Sand transport, erosion and granular electrification. *Aeolian Res.* 4, 1–16. <http://dx.doi.org/10.1016/j.aeolia.2011.12.003>.
- Middleton, N., Sternberg, T., 2013. Climate hazards in drylands: a review. *Earth-Sci. Res.* 126, 48–57. <http://dx.doi.org/10.1016/j.earscirev.2013.07.008>.
- Nalpanis, P., Hunt, J.C.R., Barret, C.F., 1993. Saltating particles over flat beds. *J. Fluid Mech.* 251, 661–685. <http://dx.doi.org/10.1017/S00221120930035568>.
- Nelsen, R.B., 2007. An Introduction to Copulas. Springer-Verlag. <http://dx.doi.org/10.1007/0-387-28678-0>.
- Niño, Y., Lopez, F., Garcia, M., 2003. Threshold for particle entrainment into suspension. *Sedimentology* 50. <http://dx.doi.org/10.1046/j.1365-3091.2003.00551.x>.
- Nicking, W.G., McKenna Neuman, N.C., 1997. Wind tunnel evaluation of a wedge-shaped aeolian sediment trap. *Geomorphology* 18, 333–345. [http://dx.doi.org/10.1016/S0169-555X\(96\)00040-2](http://dx.doi.org/10.1016/S0169-555X(96)00040-2).
- Nickling, W.G., 1988. The initiation of particle movement by wind. *Sedimentology* 35, 499–511.
- Pahtz, T., Kok, J.F., Herrmann, H.J., 2012. The apparent roughness of a sand surface blown by wind from an analytical model of saltation. *New J. Phys.* 14. <http://dx.doi.org/10.1088/1367-2630/14/4/043035>.
- Poortinga, A., Keijsers, J.G., Maroulis, J., Visser, S.M., 2014. Measurement uncertainties in quantifying aeolian mass flux: evidence from wind tunnel and field site data. *PeerJ* 2, e454. <http://dx.doi.org/10.7717/peerj.454>.
- Pye, K., Tsaoar, H., 2009. Aeolian Sand and Sand Dunes. Springer. <http://dx.doi.org/10.1007/978-3-540-85910-9>.
- Rasmussen, K., Iversen, J., Rautahemio, P., 1994. The effect of surface slope on saltation threshold. *Sedimentology* 41, 7218.
- Ravi, S., Dodirico, P., Over, T., Zobeck, T.M., 2004. On the effect of air humidity on soil susceptibility to wind erosion: the case of air-dry soils. *Geophys. Res. Lett.* 31, L09501.
- Refsgaard, J.C., van der Sluijs, J.P., Hojberg, A.L., Vanrolleghem, P.A., 2007. Uncertainty in the environmental modelling process – a framework and guidance. *Environ. Model. Softw.* 22, 1543–1556.
- Regan, H.M., Colyvan, M., Burgman, M.A., 2002. A taxonomy and treatment of uncertainty for ecology and conservation biology. *Ecol. App.* 12, 618–628.
- Rizvi, A., 1989. Planning responses to aeolian hazards in arid regions. *J. King Saud Univ. Archit. Planning* 1, 59–74.
- Roney, J.A., White, B.R., 2004. Definition and measurement of dust aeolian thresholds. *J. Geophys. Res.* 109. <http://dx.doi.org/10.1029/2003JF000061>.
- Saffman, P., 1965. Lift on a small sphere in a slow shear flow. *J. Fluid Mech.* 22, 385. <http://dx.doi.org/10.1017/S0022112065000824>.
- Schölzel, C., Friederichs, P., 2008. Multivariate non-normally distributed random variables in climate research – introduction to the copula approach. *Nonlinear Processes Geophys.* 15, 761–772.
- Shao, Y., 2008. Physics and Modelling of Wind Erosion, second ed. Springer. <http://dx.doi.org/10.1007/978-1-4020-8895-7>.
- Shao, Y., Lu, H., 2000. A simple expression for wind erosion threshold friction velocity. *J. Geophys. Res.* 105, 22437–22443. <http://dx.doi.org/10.1029/2000JD900304>.
- Sherman, D., Li, B., 2012. Predicting aeolian sand transport rates: a reevaluation of models. *Aeolian Res.* 3, 371–378. <http://dx.doi.org/10.1016/j.aeolia.2011.06.002>.
- Swann, C., Ewing, R., Sherman, D., 2015. A threshold continuum for aeolian sand transport. In: Proceedings American Geophysical Union Fall Meeting, abstract EP24A-04, San Francisco.
- Tian, Y., 1988. Wind erosion: threshold velocity for initial particle movement (Master's thesis). Texas Tech University.
- Trivedi, P.K., Zimmer, D.M., 2005. Copula Modeling: An Introduction for Practitioners. volume 1. now Publisher. doi:<http://dx.doi.org/10.1561/0800000005>.
- Usitalo, L., Lehtikoinen, A., Helle, I., Myrberg, K., 2015. An overview of methods to evaluate uncertainty of deterministic models in decision support. *Environ. Model. Softw.* 63, 24–31.
- Venter, G.G., 2002. Tails of copulas. In: Proceedings of the Casualty Actuarial Society.
- de Waal, D., van Gelder, P., 2005. Modelling of extreme wave heights and periods through copulas. *Extremes* 8, 345–356. <http://dx.doi.org/10.1007/s10687-006-0006-y>.
- Webb, N., Strong, C., 2011. Soil erodibility dynamics and its representation for wind erosion and dust emission models. *Aeolian Res.* 3, 165–179. <http://dx.doi.org/10.1016/j.aeolia.2011.03.002>.
- Williams, J.J., Butterfield, G.R., Clark, A.G., 1990. Rates of aerodynamic entrainment in a developing boundary layer. *Sedimentology* 37, 1039–1048.
- Williams, J.J., Butterfield, G.R., Clark, A.G., 1994. Aerodynamic entrainment threshold: effects of boundary layer flow conditions. *Sedimentology* 41, 309–328.
- Wu, F.C., Chou, Y.J., 2003. Rolling and lifting probabilities for sediment entrainment. *J. Hydraulic Eng.* 129.
- Yan, J., Liu, Y., Han, S., Wang, Y., Feng, S., 2015. Reviews on uncertainty analysis of wind power forecasting. *Renewable Sustainable Energy Rev.* 52, 1322–1330.
- Zhang, C., Zou, X., Cheng, H., Yang, S., Pan, X., Liu, Y., Dong, G., 2007. Engineering measures to control windblown sand in shiquanhe town, tibet. *J. Wind Eng. Ind. Aerod.* 95, 53–70. <http://dx.doi.org/10.1016/j.jweia.2006.05.006>.
- Zhang, K., Chanpura, R.A., Mondal, S., Wu, C., Sharma, M.M., Ayoub, J.A., Parlar, M., 2014. Particle size distribution measurement techniques and their relevance or irrelevance to sand control design. In: Proceedings of the 2014 SPE International Symposium and Exhibition on Formation Damage Control, Lafayette, Louisiana, USA, February 26–28, 2014. Society of Petroleum Engineers.
- Zhen-shan, L., Xiao-hu, Z., Wen, H., 2008. A stochastic model for initial movement of sand grains by wind. *Earth Surface Processes Landforms* 33, 1796–1803.
- Zheng, X., 2009. Mechanics Wind-Blown Sand Movements. Springer-Verlag.
- Zimon, A.D., 1982. Adhesion of Dust and Powder. Springer. <http://dx.doi.org/10.1007/978-1-4615-8576-3>.
- Zingg, A.W., 1953. Wind tunnel studies of the movement of sedimentary material. In: Proceedings of the Fifth Hydraulic Conference. Studies in Engineering. University of Iowa, Iowa City, pp. 111–135.
- Zio, E., Pedroni, N., 2013. Literature review of methods for representing uncertainty. Foundation for an Industrial Safety Culture.